Projecting twenty-first century regional sea-level changes

Article *in* Climatic Change · March 2014

DOI: 10.1007/s10584-014-1080-9

CITATIONS
189

READS
781

7 authors, including:

Mark Carson
University of Hamburg
22 PUBLICATIONS **379** CITATIONS
SEE PROFILE

Caroline A. Katsman
Delft University of Technology
79 PUBLICATIONS **2,125** CITATIONS
SEE PROFILE

R.S.W. Van de Wal
Utrecht University
308 PUBLICATIONS **10,694** CITATIONS
SEE PROFILE

Armin Köhl
University of Hamburg
119 PUBLICATIONS **2,925** CITATIONS
SEE PROFILE

Climatic Change manuscript No.
(will be inserted by the editor)

Projecting twenty-first century regional sea-level changes

A.B.A. Slangen · M. Carson · C.A. Katsman · R.S.W. van de Wal · A. Köhl · L.L.A. Vermeersen · D. Stammer

Received: date / Accepted: date

Abstract We present regional sea-level projections and associated uncertainty estimates for the end of the 21^{st} century. We show regional projections of sea-level change resulting from changing ocean circulation, increased heat uptake and atmospheric pressure in CMIP5 climate models. These are combined with model- and observation-based regional contributions of land ice, groundwater depletion and glacial isostatic adjustment, including gravitational effects due to mass redistribution. A moderate and a warmer climate change scenario are considered, yielding a global mean sea-level rise of 0.54±0.19 m and 0.71±0.28 m respectively (mean±1σ). Regionally however, changes reach up to 30% higher in coastal regions along the North Atlantic Ocean and along the Antarctic Circumpolar Current, and up to 20% higher in the subtropical and equatorial regions, confirming patterns found in previous studies. Only 50% of the global mean value is projected for the subpolar North Atlantic Ocean, the Arctic Ocean and off the western Antarctic coast. Uncertainty estimates for each component demonstrate that the land ice contribution dominates the total uncertainty.

A.B.A. Slangen and R.S.W. van de Wal
Institute for Marine and Atmospheric research Utrecht (IMAU), Utrecht University, Princetonplein 5, 3584 CC Utrecht, The Netherlands

A.B.A. Slangen is now at
CSIRO Marine and Atmospheric Research (CMAR), GPO Box 1538, Hobart, TAS 7001, Australia
Tel.: +61 3 6232 5170
E-mail: aimee.slangen@gmail.com

M. Carson, A. Köhl and D. Stammer
Center for Earth System Research and Sustainability (CEN), University of Hamburg, Bundesstrasse 53, D-20146 Hamburg, Germany

C. A. Katsman
Royal Netherlands Meteorological Institute (KNMI), P.O. Box 201, 3730 AE De Bilt, The Netherlands

L.L.A. Vermeersen
Delft Climate Institute, Faculty of Aerospace Engineering, TU Delft, Kluyverweg 1, 2629 HS Delft, The Netherlands and Royal Netherlands Institute for Sea Research (NIOZ), Landsdiep 4, 1797 SZ 't Horntje, The Netherlands

Keywords Regional sea-level change · CMIP5 · climate change · model projections

1 Introduction

Estimating future sea-level change [SLC] is a pressing topic in climate research, with direct socio-economic consequences (Nicholls and Cazenave, 2010). Since there are many processes that contribute to SLC with spatially varying patterns (Milne et al, 2009; Willis and Church, 2012), the main challenge is to develop regional estimates, as local governments and industries have a vested interest in anticipating the degree of SLC in their vicinity.

Traditionally, sea-level research focused on global mean changes, both in reconstructing the past (e.g., Holgate and Woodworth, 2004; Church and White, 2006) and in projecting the future; either with process-based models that account for physical processes (e.g., Meehl et al, 2007b, and references therein) or with semi-empirical models (e.g., Rahmstorf, 2007). Recently however, the attention has been shifting towards understanding and projecting regional changes in sea level.

Recent publications have combined steric and dynamic sea surface height [SSH] contributions from climate models with offline calculations of the gravitational effects from land ice melt (Mitrovica et al, 2001) to project regional changes (e.g., Kopp et al, 2010; Slangen et al, 2012; Spada et al, 2013; Perrette et al, 2013). The first three studies include model data from phase 3 of the WRCP Coupled Model Intercomparison Project [CMIP3] (Meehl et al, 2007a), while the latter study also includes data from phase 5 [CMIP5] (Taylor et al, 2012), which contains the latest suite of coupled climate model results to date. Yin (2012) compares CMIP3 and CMIP5 models, and finds that the model-to-model spread in global thermosteric SSH is diminished in the newer CMIP5 ensemble, but that the spread in the pattern of dynamic SSH is not overall better in CMIP5. Other differences between the aforementioned projection studies are in the treatment of the land ice contributions or the use of a probabilistic approach (Perrette et al, 2013), which will be further discussed in Section 4.

In addition to dynamic SSH and gravitational effects resulting from land ice mass changes, other processes can influence regional sea-level changes, such as long term Glacial Isostatic Adjustment [GIA] (Peltier, 2004), terrestrial storage changes resulting from groundwater extraction (Wada et al, 2012) or reservoir building (Chao et al, 2008), and atmospheric pressure loading [AL] (Wunsch and Stammer, 1997). While these all have a relatively small global effect compared to the steric and land ice contributions, they can be of significant magnitude locally, and therefore need to be included when focusing on regional changes.

In this study, the set of sea-level contributions is expanded with respect to other studies by adding regional projections of groundwater depletion and AL. GIA is also included, as was already done in Slangen et al (2012). In contrast to other studies, we explicitly separate the contributions of the ice sheet surface mass balance [SMB] and the dynamical processes on the ice sheets, because they respond differently to climate change. While previous work (Slangen et al, 2012) showed a first estimate of the regional patterns in SLC based on global mean estimates from the Intergovernmental Panel on Climate Change Fourth Assessment Report

(IPCC AR4; Meehl et al, 2007b), here the estimates are primarily based on the newer CMIP5 climate models.

We present regional SLC projections for the end of the 21^{st} century based on an ensemble of 21 CMIP5 climate model projections. For the analysis we use the Representative Concentration Pathways [RCP] 4.5 and 8.5 scenarios (Moss et al, 2010), to assess the impacts of a moderate and a warmer climate change scenario. We combine regional projections of SLC resulting from changing ocean circulation, increased heat uptake and atmospheric pressure in the CMIP5 models with model- and observation-based contributions of land ice, groundwater depletion and GIA. The changes in glaciers and ice caps and ice sheet SMB are modelled using CMIP5 model output, while the groundwater contribution is based on CMIP3. Because the link between climate change and ice sheet dynamical processes is still an area of active research (e.g., Pritchard et al, 2012; Nick et al, 2013), there are no complete models of future changes in ice sheet dynamics available yet. We therefore construct an RCP-independent scenario for the ice dynamical contribution, which is based on two different estimates that exist in literature, using Meehl et al (2007b) as a lower bound and Katsman et al (2011) as an upper bound. This scenario does not include a possible collapse of the West-Antarctic Ice Sheet (Bamber et al, 2009; Joughin and Alley, 2011). The regional patterns for all mass redistribution components are computed while accounting for gravitational, rotational and visco-elastic deformation effects.

Combining the regional patterns of all these contributions yields a more complete estimate of regional SLC than was available before. Equally important, this study provides uncertainty measures for each contribution. Finally, we show the regional deviation from the global mean change, and identify regions that will likely experience a SLC substantially different from the global mean. All patterns shown here are relative changes, which is the change in sea level relative to the Earth's surface.

The data and models used to project the regional changes of the various contributions are described in Section 2. In Section 3, we show the global mean values, associated regional patterns and their uncertainties. This section also shows net projections of regional SLC, and describes the local deviations from the total global mean change. Section 4 provides a comparison between previous studies projecting regional SLC and the current study. Section 5 presents conclusions and open issues.

2 Data and Methods

2.1 CMIP5 Climate Models

Our analysis is based on an ensemble of 21 Atmosphere-Ocean coupled General Circulation Models [AOGCM's] from the CMIP5 archive, listed in Online Resource Table 1. The skill of these climate models in simulating the present-day sea-level pattern is shown in Online Resource Fig.1. The data used comprises 2m air temperature, precipitation, global mean thermosteric SLC, regional SSH above geoid, and sea-level pressure. All variables are interpolated onto a common $1^\circ \times 1^\circ$ grid, using bilinear interpolation with nearest-neighbor interpolation near coasts. The ocean area covered by the ensemble land-sea mask is 90% of the actual area, which is an

increase of 10% with respect to the CMIP3 ensemble. Two RCP climate change scenarios are studied: RCP4.5 with a global mean surface temperature increase of 1.2–2.7°C between 1986–2005 and 2081–2100, and RCP8.5 with an increase of 2.7–5.4°C.

2.2 Combined ocean circulation and heat uptake contribution

The combined ocean circulation and heat uptake contribution, hereafter referred to as steric+dynamic, is constructed from the CMIP5 data by adding the (time varying) global mean thermosteric SLC to the (spatially varying) SSH above the geoid. The projected fields are computed using one member of each individual model for the period 2081–2100 minus 1986–2005 by (i) removing a quadratic-fit regional control drift in each x,y grid box, (ii) subtracting the global mean at each time step so it is zero, (iii) adding the global mean thermosteric SSH time series to each grid point. These computations are made on the original model grids, with the conversion to a common 1-degree grid only done directly prior to computing a mean regional SLC field over the model ensemble. All global data are corrected for model drift by subtracting the quadratic trend in the time series of the accompanying pre-industrial control run (Gregory et al, 2001; Katsman et al, 2008). We note that due to the lack of volcanic forcing in pre-industrial control runs, this way of correcting the drift is likely to impose a bias to smaller SLC in historical runs as well as in RCP climate change scenarios (Gregory, 2010).

2.3 Atmospheric Loading [AL]

Local SLC is influenced by changes in AL (Wunsch and Stammer, 1997; Stammer and Huttemann, 2008), which result from changes in the atmospheric circulation and changes in the column-integrated atmospheric moisture content. A surface pressure decrease (increase) of 1 millibar yields a sea-level rise (drop) of approximately 0.01 m. As coupled climate models do not account for AL effects explicitly (i.e., changes in the atmospheric mass over each grid point are ignored when calculating the local SLC), AL is computed here following Stammer and Huttemann (2008).

The CMIP5 models project an increase of the globally averaged atmospheric moisture content over the 21st century, which, if it originates from the ocean, will yield a net decrease in sea level. If we assume all moisture change is due to ocean evaporation, the ensemble mean moisture change corresponds to a maximum SLC of -0.004 m (RCP4.5) and -0.009 m (RCP8.5). Compared to the other contributions this is negligible and hence omitted from our projections.

2.4 Land Ice Contribution

The land ice contribution comprises all glaciers and ice caps (henceforth “glaciers”), and the ice sheets on Greenland and Antarctica. In addition, GIA as a result of ice sheet melt after the Last Glacial Maximum [LGM] is included.

The glacier estimate is computed using CMIP5-based projections of temperature and precipitation changes over glacierized regions in combination with a glacier area inventory (Radić and Hock, 2010) in a model for glacier mass loss that is based on volume-area considerations (Bahr et al, 1997; Van de Wal and Wild, 2001). The volume-area approach is described in more detail in Slangen and van de Wal (2011).

The ice sheet contribution is split into a scenario-based SMB contribution and a scenario-independent dynamical contribution.

Presently, no studies are available which project SMB changes using the full CMIP5 model ensemble. We therefore use the SMB contributions and the global surface temperature change of the CMIP3 model ensemble in IPCC AR4 (Meehl et al, 2007b) to derive two total least squares fits (Online Resource Fig.2) for the ice sheet SMB contributions (η_{SMB}, m):

$$\eta_{SMB-Greenland} = 0.0153 \pm 0.01493 \times \delta T_{atm} - 0.00094 \quad (1)$$

$$\eta_{SMB-Antarctica} = -0.0105 \pm 0.01759 \times \delta T_{atm} - 0.0412. \quad (2)$$

These fits are combined with the projected CMIP5 global mean surface temperature change (δT_{atm}, °C) to calculate the CMIP5-SMB contribution of the ice sheets. The uncertainty estimates for the SMB contributions include the residual of the linear fit of each equation, which is very small (0.003 m for Eq.1 and 0.001 m for Eq.2), and the propagation of the much larger uncertainties in the η_{SMB}-δT_{atm} relations presented in Meehl et al (2007b) (see Online Resource for uncertainty estimation). For Greenland, the resulting SMB change (Table 1) is in range, albeit at the lower end, with results presented recently in Van Angelen et al (2013) and Fettweis et al (2013), who used output of respectively 1 and 3 CMIP5 models to drive a regional climate model [RCM]. There are no CMIP5-based results for Antarctica, but CMIP3-based SMB estimates (e.g., Krinner et al, 2007; Ligtenberg et al, 2013) fall within our range, with a tendency for a smaller sea-level fall.

Dynamical changes on the ice sheets comprise a large range of processes. Main mechanisms on Greenland are calving and melt of marine-terminating glaciers (e.g., Nick et al, 2013), meltwater percolation to the bedrock (e.g., Phillips et al, 2010), and ice flow-SMB feedback (e.g., Goelzer et al, 2013). On Antarctica, meltwater pond formation can lead to thinning and breaking up of ice shelves (e.g., Cook and Vaughan, 2010). Ice shelves may also melt from below when changes in circulation cause warmer water to enter onto the continental shelf (e.g., Pritchard et al, 2012), resulting in grounding line retreat.

Although the understanding of ice dynamical processes has improved in recent years, modelling is still in its early stages and comprehensive process-based future projections cannot be provided yet. For this contribution we therefore construct an RCP-independent scenario that is bound by two different estimates that exist in the literature, such that it reflects a relatively wide range of possibilities. As the lower bound for the scenario we take the scaled-up estimate of IPCC AR4 (Meehl et al, 2007b), which assumes that observed changes in the period 1993-2003 will continue but not accelerate. As the upper bound of our scenario we use the estimates presented in Katsman et al (2011), assuming a continued observed discharge in the Amundsen Sea Embayment and East Antarctica, and retreating ice shelves near tidewater glaciers in Greenland. These values are in line with estimates of

Pfeffer et al (2008), which are based on changes in discharge in potentially vulnerable areas. Recent studies in Greenland Nick et al (2013) project a contribution of 0.040–0.085 m from calving glaciers only, which is well within our range (0.01–0.11 m) and leaves room for other dynamical contributions. For Antarctica, the upper bound of our dynamical scenario (0.15 m) is in line with a recently published upper bound of 0.13 m (Little et al, 2013), who used a probabilistic framework to combine expert opinions with observational and model-based constraints.

The dynamical estimate used (Table 1) is the average of the lower and upper bounds, and we take the unbiased standard deviation as the uncertainty. The bounds are chosen to represent the most plausible range of changes, and therefore do not include high-end values associated with a West-Antarctic ice sheet collapse, since timing, speed and magnitude of this event are still highly uncertain (Bamber et al, 2009; Joughin and Alley, 2011).

In addition to the present-day land ice contributions, we include the relative SLC from the ICE5G model (Peltier, 2004) to account for deformation of the solid Earth as a result of ice melt since the LGM. GIA is a viscous effect, acting on long timescales, and is assumed to be constant over the short period considered here and thus independent from climate scenarios or models.

2.5 Groundwater Depletion

Recent studies suggest that groundwater depletion [GD] will increase in the 21^{st} century (Konikow, 2011; Wada et al, 2012), while dam building is levelling off (Chao et al, 2008). We will therefore, for the first time, include projections of GD as a regional sea-level contribution. The projections are based on data from Wada et al (2012), who provide a flux-based estimate of the difference between groundwater extraction and recharge for two CMIP3 climate models, using two different socio-economic projections in combination with population change. The projected future increase in GD is due to a decrease in the availability of surface water and a decrease in groundwater recharge, but increasing water demand for irrigation. Changes in both population and climate are important factors, which cannot be unraveled and we therefore assume that all four provided model outcomes have a similar probability of occurrence in each of the RCP scenarios. The four contributions project 0.07–0.09 m SLC, which results in a climate-scenario independent contribution of 0.08 m.

2.6 Modelling Mass Redistribution

The contributions from land ice and groundwater will not cause a uniform sea-level rise. Instead, gravitational, rotational and viscoelastic deformation effects (e.g., Mitrovica et al, 2001) need to be taken into account. The SLC patterns are computed using a model which solves the sea-level equation with a pseudo-spectral approach (Farrell and Clark, 1976; Mitrovica and Peltier, 1991; Schotman and Vermeersen, 2005), by considering changes in the Earth's gravitational field, resulting solid-earth deformation and changes in the Earth's rotation vector. The Earth model used is based on PREM (Dziewonski and Anderson, 1981), and is elastic, compressible and radially stratified. The sea-level model uses an iterative

process to compute the new state of the ocean surface after a mass change, by computing the depression of the Earth's crust, the resulting changes in the gravity field and rotation properties of the Earth, and again a redistribution of ocean mass. As a result, the model yields distinct regional patterns of SLC with a fall close to areas of mass loss, and rise for regions further away.

3 Results

3.1 Two Scenarios

We present two scenarios, which are based on RCP climate change scenarios. **Scenario A** combines CMIP5-RCP4.5 based estimates of the steric+dynamic contribution, AL, glacier and ice sheet SMB contributions with the three scenario-independent terms: the dynamical ice sheet contribution, groundwater depletion and GIA. **Scenario B** adds CMIP5-RCP8.5 based estimates of the steric+dynamic contribution, AL, glacier and ice sheet SMB contributions to the three scenario-independent terms. Scenario A yields a net global mean SLC of 0.54±0.19 m between 1986–2005 and 2081–2100, while scenario B yields 0.71±0.28 m for the same period (Table 1, mean±1σ).

3.2 Regional Contributions and Uncertainties

The ensemble mean regional patterns of the CMIP5-based land ice contributions from glaciers and ice sheet SMB (Figs.1a (RCP4.5) and 1b (RCP8.5)) have a pronounced gravitational signature (Mitrovica et al, 2001), resulting in sea-level fall near ice loss regions, sea-level rise near mass gain regions and an above-average SLC at low latitudes. Both patterns show melt on Greenland and on glaciers at high northern latitudes. Antarctica also contributes to the SLC pattern, with mass loss on the Antarctic Peninsula and mass gain in other areas of the ice sheet. The land ice contribution for RCP8.5 is larger in amplitude, resulting in SLC up to 0.24±0.18 m in equatorial regions, compared to 0.14±0.10 m for RCP4.5. The uncertainties in these climate-model dependent ice components (Figs.2a,b) are based on the spread in the CMIP5 ensemble, plus, for the SMB component, the uncertainties in the fitted slopes in Eqs.1 and 2. The uncertainties are largest near the melt sources, and therefore most prominent in regions around the Arctic Ocean and around Antarctica. Another local maximum can be seen in the far-field regions around the equator.

Figures 1c and 1d show the ensemble mean dynamic SLC patterns plus the global mean steric change for the two scenarios, including AL. The figures show substantial small-scale variability resulting from ocean dynamics, due to changing wind forcing and changes in the ocean heat and freshwater content. Regionally, steric+dynamic SLC ranges from 0.02 to 0.41 m for RCP4.5 (global mean 0.19±0.06 m), and from -0.03 to 0.59 m for RCP8.5 (global mean 0.28±0.08 m). The AL effect is much smaller: for RCP4.5 the contribution ranges from -0.01 m at low latitudes to 0.02 m at high latitudes, while for RCP8.5 the values vary between -0.03 cm and 0.05 cm. Both figures show fairly similar patterns, with higher values for RCP8.5 than for RCP4.5. In the Arctic, an above-average sea-level rise

is projected, which was also described by Landerer et al (2007), and attributed to freshening of the ocean water due to increased precipitation and river runoff. The North Atlantic displays a tripolar pattern, which Landerer et al (2007) associated with a northward shift of the North Atlantic Current after having examined changes in near-surface horizontal velocities. Yin et al (2009) attributed the pattern of the dynamic adjustment of SSH in the North Atlantic, and particularly the rise on the northeast coast of the United States, to a weakening meridional overturning circulation in the Atlantic Ocean. The Southern Ocean shows a dipolar pattern with below average increase in the south and above average increase to the north. Although low thermal expansion coefficients for colder temperatures seem to motivate the meridional gradient across the Antarctic Circumpolar Current [ACC], these changes also require a dynamical balance. In response to doubling CO2, climate models show that wind stress intensifies and the position of zero wind stress curl in the mid-latitudes of the Southern Hemisphere shifts poleward (Fyfe and Saenko, 2006), leading to a strengthening and southward shift of the ACC (Bi et al, 2002). The Southern Ocean dipole is found in most of the individual members of the model ensemble, as shown in Online Resource Fig.3. The figure also reveals large differences between the models, both in amplitude and in regional pattern. Online Resource Fig.4 shows that for the majority of the ocean surface the ratio of the two scenarios is close to 1.5, which scales with the ratio of the global mean values. However, some locations show deviating values, such as in the South Pacific Ocean, a region associated with the ACC. If the SLC would respond linearly to warming, those differences would not appear; this highlights the importance of the adjusted ocean circulation in modifying the regional heat and freshwater content of the ocean, and thereby the regional sea level.

The uncertainty in the steric+dynamic patterns including AL (Figs.2c,d) is calculated from the 21-member CMIP5 model ensemble RMS spread. Both show a high spatial variability, similar to the ensemble mean values. The figures show that the uncertainties are largest where the ensemble mean pattern shows the largest deviations from the global mean. The largest uncertainties are found in the Arctic region, which is associated with differences in the timing of the reduction of the sea ice. The AL uncertainties are small compared to the steric+dynamic contribution, with maximum values of 0.016 m for RCP4.5 and 0.022 m for RCP8.5. This is large relative to the values of the ensemble mean AL pattern, but small compared to other uncertainties.

The scenario-independent dynamical ice sheet contribution (Fig.1e) yields a regional pattern showing sea-level fall in the vicinity of both ice sheets, and sea-level rise in the midlatitude and tropical regions, amplifying the pattern caused by the climate-dependent land ice contributions. The uncertainty estimate of the ice-dynamical scenario (see Section 2.4) is largest near the two ice sheets (Fig.2e), but also displays a considerable value in the low latitudes. Since the regions of mass loss are similar to those for the climate-dependent land ice contribution, the ice dynamics amplify the uncertainty that results from these contributions.

Similar to land ice, the groundwater contribution also yields a gravitational pattern (Fig.1f), because water mass is redistributed from land to ocean. Most of the depletion occurs in (semi)arid regions, which is expected to increase in the future due to increasing irrigation demand. This is reflected by the regional pattern, showing a sea-level fall close to areas with large depletion, e.g. near the USA, India, the middle East and also in Europe. The uncertainty in this contribution

is calculated from the 4-member ensemble RMS spread. Similar to the land ice uncertainties, Fig.2f shows that the uncertainties are largest near the sources of groundwater extraction.

The scenario-independent GIA contribution is shown in Fig.1g. Although GIA is mostly small, it plays an important role near regions where large ice sheets used to be during the LGM, such as for instance near Scandinavia or around the North American continent. Estimating the uncertainty in the GIA contribution is challenging (Hanna et al, 2013, Box 1), because there are no statistical errors available for this type of models. We therefore estimate a systematical error, which we treat as a standard error for the purpose of combining it with the other uncertainties, by taking the absolute difference between two GIA-models, using results from ICE5G (Peltier, 2004) and ANU (Nakada and Lambeck, 1988, updated in 2004-2005). The uncertainties (Fig.2g) are largest near the main GIA regions, and reflect the differences in LGM ice sheet extent and viscosity profiles between the two estimates.

3.3 Net Projections and Uncertainties

The net projected SLC pattern is considerably larger for scenario B (Fig.3b) than for scenario A (Fig.3a). In both scenarios, we observe high spatial variability due to the steric+dynamic contribution, but also sea-level fall resulting from land ice melt around Greenland and Western Antarctica, as well as GIA effects in the Barents Sea. For the computation of the net uncertainty, in Figs.3c and 3d, the uncertainties for CMIP5-contributions are assumed to be dependent, while uncertainties from all other contributions are assumed independent. Although the 90% confidence level uncertainties are of considerable magnitude, the signal is larger than the uncertainty in nearly all regions for both scenarios, particularly at middle to low latitudes where human habitation is highest. The dynamic ice sheet contribution dominates the local uncertainty, followed by steric+dynamic and ice sheet SMB uncertainties, which both are of the same order of magnitude. Smaller uncertainty contributions result from glaciers, groundwater depletion, GIA and AL. For all components, the absolute values for the scenario B uncertainties are larger than for scenario A, although this is not the case for the signal-to-noise ratios.

The distribution function of the total local SLC (Fig.4a) is slightly skewed. For both scenarios, it reveals significant regional deviations from the global mean with a longer tail towards lower values, and an upper limit that is set by the gravitational effect on the land ice and groundwater contributions. In both cases, the mode of the distribution function is above the global average. This is a consequence of the gravitational pattern associated with the land ice contribution, which yields a relatively small ocean area with low SLC values near ice loss regions, and a relatively large ocean area in the equatorial region with SLC values slightly above average.

The relative deviation of the local SLC with respect to the global mean is shown in Fig.4b. Locally, SLC deviates more than 10% and 25% from the global mean projection for up to 30% and 9% of the ocean area, respectively. Regionally, values of up to 30% above the global mean are reached, for instance in the equatorial regions, around Australia, at the southern African coast, and around North

America. We find relatively low values down to only 50% of the global mean in the Arctic region and near the coasts of South America. Although the combined values are larger for Scenario B, the relative deviation from the global mean is mostly similar for both scenarios, and many regions are likely to experience a regional SLC that differs substantially from the global mean. All contributions may cause these deviations, as shown in Online Resource Fig.5.

4 Discussion

In all recent studies on regional sea-level projections (Slangen et al (2012)[SL12], Spada et al (2013)[SP13], Perrette et al (2013)[P13]), the land ice contributions are treated differently. SP13 used RCM output for the ice sheet contributions, and a regional mass balance model for the glaciers. This was done for one climate model and one scenario only, because ice sheet RCMs are too computationally expensive to be used for a large ensemble. P13 used two scenarios for ice sheet melt: one AR4 based and the other a semi-empirical estimate. For the glacier contribution, they assumed a global mean SMB sensitivity, which cannot account for glaciers diminishing completely. The global mean ice contributions were translated into a SLC pattern with a fixed spatial melt distribution, which does not consider spatial and temporal variations that may occur due to temperature and precipitation differences. SL12 and the present study use the volume-area approach for glaciers, with CMIP3 and CMIP5 data, respectively. The ice sheet SMB contribution in SL12 was based on Gregory and Huybrechts (2006), who combined annual CMIP3 temperature and precipitation time series with spatial data from 4 high-resolution models to derive empirical equations for each climate model. Because there are no such relations available for CMIP5, we derived a relation between SMB and temperature from IPCC AR4, and applied this to CMIP5 temperature data to obtain SMB estimates. In both studies, the ice sheet dynamical contribution is treated separately. SL12 followed IPCC AR4, while here we have constructed a scenario bound by two independent estimates.

While SP13, SL12 and this study model the regional patterns for each contribution, climate model and scenario separately, P13 used probabilistic projections of global mean change, and scaled these for each contribution using contribution-specific fingerprints. By doing this, P13 assume that fingerprints will not change in time or for varying temperature change. For the steric+dynamic contribution we show in Online Resource Fig.4 that temperature scaling does not work everywhere, thereby stressing the need of regional projections for each climate scenario.

Despite the differences identified above, there are also some similarities. All studies highlight the fact that it is critical to include gravitational effects, since these will largely determine future SLC patterns. Another common feature is an above-average SLC in the equatorial oceans due to the combination of above-average steric+dynamic sea-level rise and a far-field effect as a result of melting ice in the polar regions. This general pattern is robust across all studies, although the exact magnitude is not agreed upon and heavily depends on the magnitude of the ice sheet contributions.

5 Conclusions

In this study we have shown the most complete sea-level projections to date, highlighting the fact that it is important to consider regional changes in sea level for planning purposes. The projections shown here are based on the state-of-the-art climate model database (CMIP5), and, relative to earlier CMIP3-based estimates (Slangen et al, 2012), on a larger model ensemble. An important addition with respect to previous studies is the groundwater contribution (Wada et al, 2012), which could not be added before, because no projections were available. In addition, an AL correction is included (Stammer and Huttemann, 2008), which is not included in the ocean component of coupled climate models in the CMIP5 database (S. Griffies, pers.comm.). Using the new climate model data, combined with regional estimates for contributions from land ice, groundwater depletion and GIA, we project new regional sea-level patterns. We find regional variations in sea-level up to 30% above and 50% below the global mean. SLC well above the global mean is projected for the equatorial oceans, because these are the far-field regions of the land ice melt contribution, in combination with an average to above-average steric+dynamic change. SLC below the global mean is projected for the Arctic Ocean, the regions around both ice sheets and main sources of land ice melt. Because all the individual contributions to SLC can dominate locally, continued research is needed on the regional patterns of all the separate components, and to determine the causes of these local variations.

Future improvements to regional SLC projections are anticipated by incorporating the effects of fresh water release from land ice melt and groundwater depletion on ocean dynamics. 50-year model simulations carried out for a steady Greenland melting of about 2 mm/year (Stammer et al, 2011) are a first step in that direction. They suggest that this effect is important for regional sea level, as regional steric changes are found to raise sea level by as much as 0.15 m in the subpolar North Atlantic Ocean. However, to be able to quantify the impact on regional SLC in a consistent way, coupled climate model simulations are required in which a freshwater contribution is applied that matches the pattern and amplitude of the combined (range of) projected rates of total land ice melt and groundwater depletion for the 21^{st} century. Such simulations are not yet available, but highly desirable.

Acknowledgements We thank Y. Wada and M. Bierkens for the groundwater depletion data, and R. Riva and P. Stocchi for the GIA data. We thank 3 reviewers for commenting on the manuscript. We acknowledge the WRCP's Working Group on Coupled Modeling, which is responsible for CMIP, and we thank the climate modeling groups listed in OR-Table 1 for producing and making available their model output. MSS_CNES_CLS11 was produced by CLS Space Oceanography Division and distributed by AVISO, with support from CNES (http:www.aviso.oceanobs.com). A.S. is supported by SRON (ALW-GO-AO/07-14). M.C. and D.S. are supported through the DFG funded CLISAP excellence initiative.

References

Bahr DB, Meier MF, Peckham SD (1997) The physical basis of glacier volume-area scaling. J Geophys Res 102(B9):20,355–20,362

Bamber JL, Riva REM, Vermeersen LLA, LeBrocq AM (2009) Reassessment of the Potential Sea-Level Rise from a Collapse of the West Antarctic Ice Sheet. Science 324:901–903

Bi D, Budd WF, Hirst AC (2002) Response of the antarctic circumpolar current transport to global warming in a coupled model. Geophys Res Lett 29(24), DOI 10.1029/2002GL015919
Chao BF, Wu YH, Li YS (2008) Impact of Artificial Reservoir Water Impoundment on Global Sea Level. Science 320:212–214, DOI 10.1126/science.1154580
Church JA, White NJ (2006) A 20th century acceleration in global sea-level rise. Geophys Res Lett 33:L01,602, DOI 10.1029/2005GL024826
Cook AJ, Vaughan DG (2010) Overview of areal changes of the ice shelves on the Antarctic Peninsula over the past 50 years. The Cryosphere 4:77–98, DOI 10.5194/tc-4-77-2010
Dziewonski AM, Anderson DL (1981) Preliminary reference Earth model. Phys Earth Planet Inter 25:297–356
Farrell WE, Clark JA (1976) On Postglacial Sea Level. Geophys J R Astron Soc 46:647–667
Fettweis X, Franco B, Tedesco M, van Angelen JH, Lenaerts JTM, van den Broeke MR, Gallee H (2013) Estimating the Greenland ice sheet surface mass balance contribution to future sea level rise using the regional atmospheric climate model MAR. The Cryosphere 7:469–489, DOI 10.5194/tc-7-469-2013
Fyfe JC, Saenko OA (2006) Simulated changes in the extratropical Southern Hemisphere winds and currents. Geophys Res Lett 33(6), DOI 10.1029/2005GL025332
Goelzer H, Huybrechts P, Fürst JJ, Nick FM, Andersen ML, Edwards TL, Fettweis X, Payne AJ, Shannon S (2013) Sensitivity of Greenland ice sheet projections to model formulations. Journal of Glaciology 59(216), DOI 10.3189/2013JoG12J182
Gregory JM (2010) Long?term effect of volcanic forcing on ocean heat content. Geophys Res Lett 37(L22701), DOI 10.1029/2010GL045507
Gregory JM, Huybrechts P (2006) Ice-sheet contributions to future sea-level change. Phil Trans R Soc A 364(doi:10.1098/rsta.2006.1796):1709–1731
Gregory JM, Church JA, Boer GJ, Dixon KW, Flato GM, Jackett DR, Lowe JA, O'Farrell SP, Roeckner E, Russell GL, Stouffer RJ, Winton M (2001) Comparison of results from several aogcms for global and regional sea level change 1900-2100. Climate Dynamics 18:225–240
Hanna E, Navarro FJ, Pattyn F, Domingues CM, Fettweis X, Ivins ER, Nicholls RJ, Ritz C, Smith B, Tulaczyk S, Whitehouse PL, Zwally HJ (2013) Ice-sheet mass balance and climate change. Nature 498(7452):51–59, DOI 10.1038/nature12238
Holgate SJ, Woodworth PL (2004) Evidence for enhanced coastal sea level rise during the 1990s. Geophys Res Lett 31:L07,305, DOI 10.1029/2004GL019626
Joughin I, Alley RB (2011) Stability of the West Antarctic ice sheet in a warming world. Nature Geoscience 4:506–513, DOI 10.1038/ngeo1194
Katsman CA, Hazeleger W, Drijfhout SS, van Oldenborgh GJ, Burgers G (2008) Climate scenarios of sea level rise for the northeast Atlantic Ocean: a study including the effects of ocean dynamics and gravity changes induced by ice melt. Climatic Change 91(3):351–374, DOI 10.1007/s10584-008-9442-9
Katsman CA, Sterl A, Beersma JJ, van den Brink HW, Church JA, Hazeleger W, Kopp RE, Kroon D, Kwadijk J, Lammersen R, Lowe J, Oppenheimer M, Plag HP, Ridley J, von Storch H, Vaughan DG, Vellinga P, Vermeersen LLA, van de Wal RSW, Weisse R (2011) Exploring high-end scenarios for local sea level rise to develop flood protection strategies for a low-lying delta—the Netherlands as an example. Clim Change 109:617–645, DOI 10.1007/s10584-011-0037-5
Konikow LF (2011) Contribution of global groundwater depletion since 1900 to sea?level rise. Geophys Res Lett 38(L17401), DOI 10.1029/2011GL048604
Kopp RE, Mitrovica JX, Griffies SM, Yin J, Hay CC, Stouffer RJ (2010) The impact of Greenland melt on local sea levels: a partially coupled analysis of dynamic and static equilibrium effects in idealized water-hosing experiments. Clim Change 103:619–625, DOI 10.1007/s10584-010-9935-1
Krinner G, Magand O, Simmons I, Genthon C, Dufresne JL (2007) Simulated Antarctic precipitation and surface mass balance at the end of the twentieth and twenty-first centuries. Clim Dyn 28:215–230, DOI 10.1007/s00382-006-0177-x
Landerer FW, Jungclaus JH, Marotzke J (2007) Regional dynamic and steric sea level change in response to the IPCC-A1B scenario. J Phys Oceanogr 37(296-312)
Ligtenberg SRM, van de Berg WJ, van den Broeke MR, Rae JGL, van Meijgaard E (2013) Future surface mass balance of the Antarctic ice sheet and its influence on sea level change, simulated by a regional atmospheric climate model. Clim Dyn 41:867–884, DOI 10.1007/s00382-013-1749-1

Little CM, Oppenheimer M, Urban NM (2013) Upper bounds on twenty-first-century Antarctic ice loss assessed using a probabilistic framework. Nature Clim Change 3:654–659, DOI 10.1038/nclimate1845

Meehl GA, Covey C, Delworth T, Latif M, McAvaney B, Mitchell JFB, Stouffer RJ, Taylor KE (2007a) The WCRP CMIP3 multi-model dataset: A new era in climate change research. Bull Am Meteorol Soc 88:1383–1394

Meehl GA, Stocker TF, Collins WD, Friedlingstein P, Gaye A, Gregory J, Kitoh A, Knutti R, Murphy J, Noda A, Raper S, Watterson I, Weaver A, Zhao ZC (2007b) Global Climate Projections. In: Climate Change 2007: The Physical Science Basis. Contribution of Working Group I to the Fourth Assessment Report of the Intergovernmental Panel on Climate Change [Solomon, S., D. Qin, M. Manning, Z. Chen, M. Marquis, K.B. Averyt, M. Tignor and H.L. Miller (eds.)], Cambridge University Press, Cambridge, U. K. and New York, NY. USA

Milne GA, Gehrels WR, Hughes CW, Tamisiea ME (2009) Identifying the causes of sea-level change. Nature geoscience 2:471–478, DOI 10.1038/NGEO544

Mitrovica JX, Peltier WR (1991) On Postglacial Geoid Subsidence Over the Equatorial Oceans. J Geophys Res 96(B12):20,053–20,071

Mitrovica JX, Tamisiea ME, Davis JL, Milne GA (2001) Recent mass balance of polar ice sheets inferred from patterns of global sea-level change. Nature 409:1026–1029

Moss RH, Edmonds JA, Hibbard KA, Manning MR, Rose SK, van Vuuren DP, Carter TR, Emori S, Kainuma, M T Kram, Meehl GA, Mitchell JFB, Nakicenovic, N K Riahi, Smith SJ, Stouffer RJ, Thomson AM, Weyant JP, Wilbanks TJ (2010) The next generation of scenarios for climate change research and assessment. Nature 463(747-756), DOI 10.1038/nature08823

Nakada M, Lambeck K (1988) The melting history of the late Pleistocene Antarctic ice sheet. Nature 333:36–40

Nicholls RJ, Cazenave A (2010) Sea-Level Rise and Its Impact on Coastal Zones. Science 328(5985):1517–1520, DOI 10.1126/science.1185782

Nick FM, Vieli A, Andersen ML, Joughin I, Payne A, Edwards TL, Pattyn F, Van de Wal RSW (2013) Future sea-level rise from Greenland's main outlet glaciers in a warming climate. Nature 497(7448), DOI 10.1038/nature12068

Peltier W (2004) Global Glacial Isostasy and the Surface of the Ice-Age Earth: The ICE-5G (VM2) Model and GRACE. Annu Rev Earth Planet Sci 32:111–149

Perrette M, Landerer F, Riva R, Frieler K, Meinshausen M (2013) A scaling approach to project regional sea level rise and its uncertainties. Earth Syst Dynam Discuss 4:11–29, DOI 10.5194/esd-4-11-2013

Pfeffer WT, Harper JT, O'Neel S (2008) Kinematic Constraints on Glacier Contributions to 21st-Century Sea-Level Rise. Science 321(1340), DOI 10.1126/science.1159099

Phillips T, Rajaram H, Steffen K (2010) Cryo-hydrologic warming: A potential mechanism for rapid thermal response of ice sheets. Geophys Res Lett 37(20), DOI 10.1029/2010GL044397

Pritchard HD, Ligtenberg SRM, Fricker HA, Vaughan DG, van den Broeke MR, Padman L (2012) Antarctic ice-sheet loss driven by basal melting of ice shelves. Nature 484(7395), DOI 10.1038/nature10968

Radić V, Hock R (2010) Regional and global volumes of glaciers derived from statistical up-scaling of glacier inventory data. J Geophys Res 115(F01010), DOI 10.1029/2009JF001373

Rahmstorf S (2007) A Semi-Empirical Approach to Projecting Future Sea-Level Rise. Science 315(5810):368–370, DOI 10.1126/science.1135456

Schotman HHA, Vermeersen LLA (2005) Sensitivity of glacial isostatic adjustment models with shallow low-viscosity earth layers to the ice-load history in relation to the performance of GOCE and GRACE. Earth and Planetary Science Letters 236:828–844

Slangen ABA, van de Wal RSW (2011) An assessment of uncertainties in using volume-area modelling for computing the twenty-first century glacier contribution to sea-level change. The Cryosphere 5:673–686, DOI 10.5194/tc-5-673-2011

Slangen ABA, Katsman CA, van de Wal RSW, Vermeersen LLA, Riva REM (2012) Towards regional projections of twenty-first century sea-level change based on ipcc sres scenarios. Clim Dyn 38(5-6):1191–1209, DOI 10.1007/s00382-011-1057-6

Spada G, Bamber JL, Hurkmans RTWL (2013) The gravitationally consistent sea-level fingerprint of future terrestrial ice loss. Geophys Res Lett 40:1–5, DOI 10.1029/2012GL053000

Stammer D, Huttemann S (2008) Response of Regional Sea Level to Atmospheric Pressure Loading in a Climate Change Scenario. J Clim 21:2093–2101, DOI 10.1175/2007JCLI1803.1

Stammer D, Agarwal N, Herrmann P, Köhl A, Mechoso CR (2011) Response of a Coupled Ocean–Atmosphere Model to Greenland Ice Melting. Surv Geophys 32:621–642, DOI

10.1007/s10712-011-9142-2
Taylor K, Stouffer RJ, Meehl GA (2012) An overview of CMIP5 and the experiment design. Bull Am Meteorol Soc 93(4):485–498, DOI 10.1175/BAMS-D-11-00094.1
Van Angelen JH, Lenaerts JTM, Van den Broeke MR, Van Meijgaard E (2013) Rapid loss of firn pore space accelerates 21st century greenland mass loss. Geophys Res Lett 40(10):2109–2113, DOI 10.1002/grl.50490
Van de Wal RSW, Wild M (2001) Modelling the response of glaciers to climate change by applying volume-area scaling in combination with a high resolution GCM. Clim Dyn 18:359–366
Wada Y, van Beek LPH, Weiland FCS, Chao BF, Wu YH, Bierkens MFP (2012) Past and future contribution of global groundwater depletion to sea-level rise. Geophys Res Lett 39(L09402), DOI doi:10.1029/2012GL051230
Willis JK, Church JA (2012) Regional Sea-Level Projection. Science 336(6081):550–551, DOI 10.1126/science.1220366
Wunsch C, Stammer D (1997) Atmospheric loading and the oceanic "inverted barometer" effect. Rev Geophys 35(1):79–107
Yin J (2012) Century to multi-century sea level rise projections from CMIP5 models. Geophys Res Lett 39(17), DOI 10.1029/2012GL052947
Yin J, Schlesinger ME, Stouffer RJ (2009) Model projections of rapid sea-level rise on the northeast coast of the United States. Nature Geoscience 2:262–266, DOI 10.1038/ngeo462

Table 1 Projected global mean$\pm 1\sigma$ SLC (m) per contribution for scenarios A and B over the period 1986–2005 to 2081–2100. Global mean contributions of GIA and AL are zero by definition and therefore excluded from this Table. [a]CMIP5-based. [b]Independent of climate scenario. [c]CMIP3-based.

	Scenario A		Scenario B	
Steric+Dynamic[a]		0.19 ± 0.06		0.28 ± 0.08
Glaciers[a]		0.15 ± 0.03		0.22 ± 0.04
Ice Sheets - SMB[a]		-0.03 ± 0.06		-0.02 ± 0.12
- *AIS*	-0.06 ± 0.03		-0.08 ± 0.07	
- *GIS*	0.03 ± 0.03		0.06 ± 0.06	
Ice Sheets - Dynamics[b]		0.15 ± 0.11		0.15 ± 0.11
- *AIS*	0.09 ± 0.06		0.09 ± 0.06	
- *GIS*	0.06 ± 0.05		0.06 ± 0.05	
Groundwater[b,c]		0.08 ± 0.01		0.08 ± 0.01
Total		0.54 ± 0.19		0.71 ± 0.28

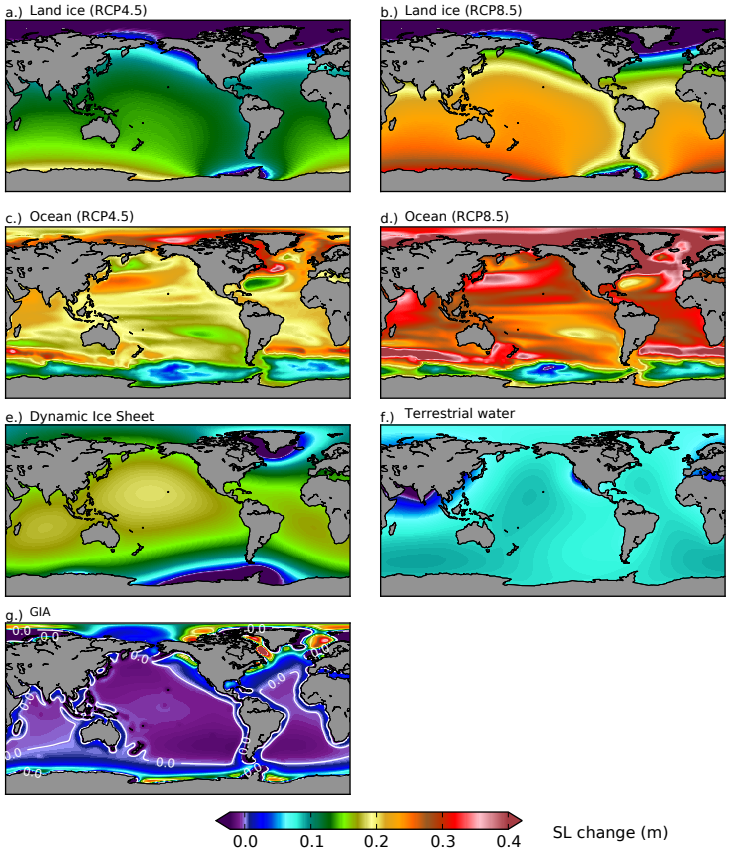

Fig. 1 Projected relative SLC patterns (m) of individual contributions over the period 1986–2005 to 2081–2100; **(a.)** RCP4.5 glaciers + ice sheet SMB, **(b.)** RCP8.5 glaciers + ice sheet SMB, **(c.)** RCP4.5 global steric+dynamic topography + AL, **(d.)** RCP8.5 global steric+dynamic topography + AL, **(e.)** Ice sheet dynamics (scenario-independent), **(f.)** Groundwater depletion (scenario-independent), **(g.)** GIA (scenario-independent). Global mean values in Table 1.

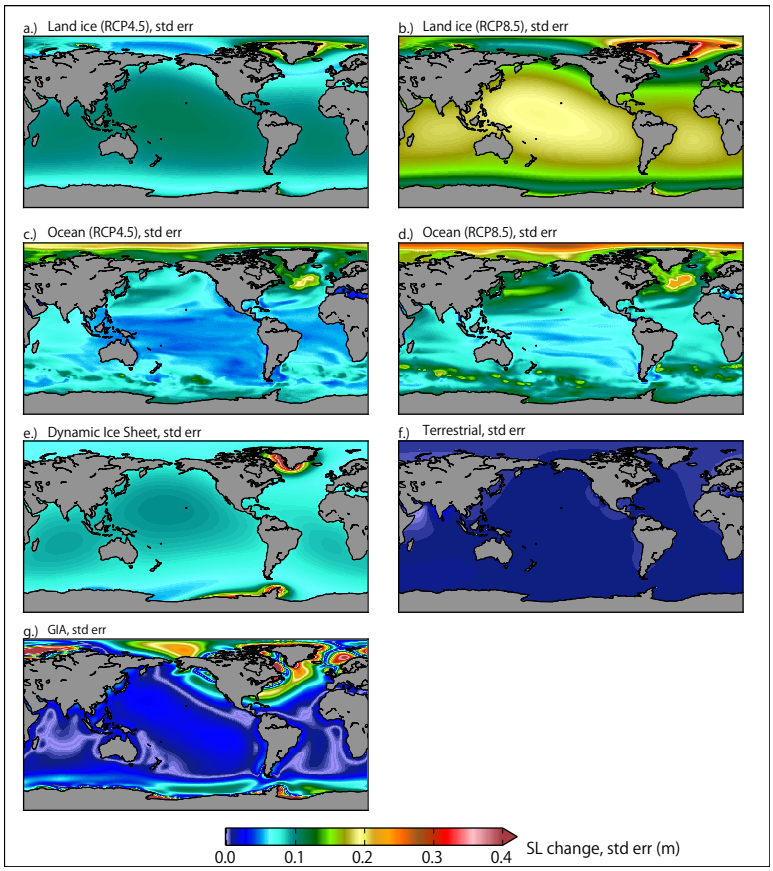

Fig. 2 Uncertainties (1σ) of projected relative SLC patterns (m) of individual contributions over the period 1986–2005 to 2081–2100; **(a.)** RCP4.5 glaciers + ice sheet SMB, **(b.)** RCP8.5 glaciers + ice sheet SMB, **(c.)** RCP4.5 global steric+dynamic topography + AL, **(d.)** RCP8.5 global steric+dynamic topography + AL, **(e.)** Ice sheet dynamics, **(f.)** Groundwater depletion, **(g.)** GIA. Global mean uncertainties in Table 1.

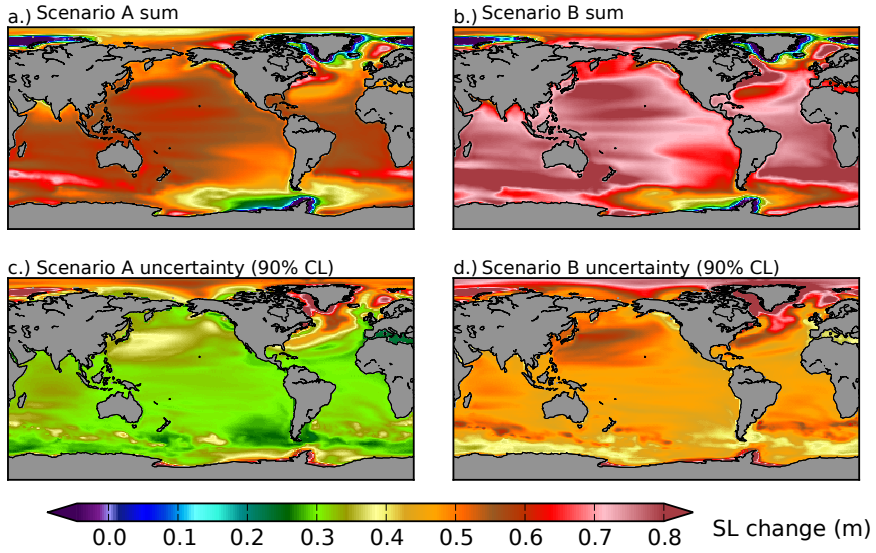

Fig. 3 Combined regional SLC patterns and uncertainties over the period from 1986–2005 to 2081–2100 for **(a.)** Scenario A sum (=Fig.1a+c+e+f+g, global mean is 0.54 m), **(b.)** Scenario B sum (=Fig.1b+d+e+f+g, global mean is 0.71 m), **(c.)** Scenario A uncertainties at the 90% confidence level (global mean is 0.32 m), **(d.)** Scenario B uncertainties at the 90% confidence level (global mean is 0.48 m).

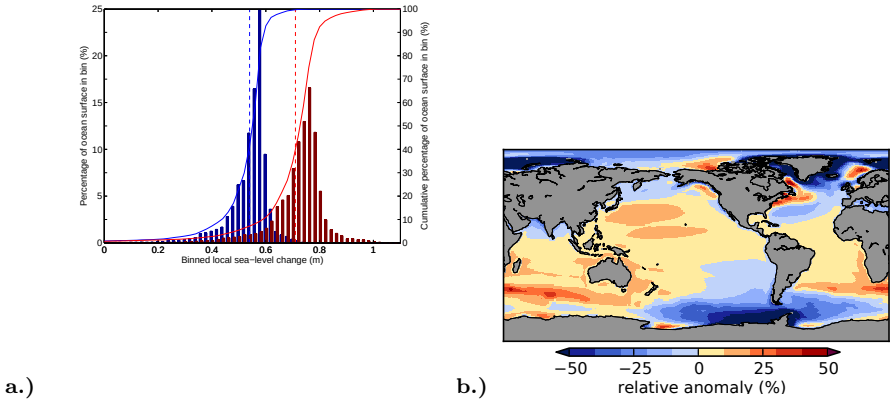

Fig. 4 **(a.)** Histogram of the binned local SLC (% of the total ocean surface, left axis); scenario A (blue), scenario B (red). Dashed lines indicate the global mean (0.54 and 0.71, respectively), solid lines the cumulative percentage (right axis). Bin width is 0.02 m. Percentage of ocean surface with less than 0 m SLC is 0.49% (A) and 0.37% (B), there are no values over 1.1 m. **(b.)** Scenario A relative SLC anomaly w.r.t. the global mean (%) between 1986–2005 and 2081–2100